[1]Hussain Mehboob

[2]Dr. Abbas Uğurenevr

Performance Evaluation of P&O, ANN and ANFIS Based MPPT Controllers of PV Array Under Partial Shading Effect in South Pole and Leading Solar Sites

Journal of Electrical Systems

Abstract: - Fuel oil is a primary source used by the research stations located at Antarctica. However, shipping fuel oil to this remote region is costly and harms the environment. Due to global warming, it has become a necessity to implement green energy technologies. Due to the nonlinear nature of PV cells and their dependence on solar irradiation and temperature, obtaining maximum power is a challenge. The system must be optimized to obtain the maximum power using Power Electronics. One way of achieving this is called Maximum Power Point Tracking (MPPT). Our research evaluates the performance of conventional method, Perturb and Observe (P&O) based MPPT technique, with modern techniques, Artificial Neural Network (ANN) and Adaptive neuro-fuzzy inference system (ANFIS) based MPPT techniques. Simulations of the ANN, ANFIS and P&O algorithms were carried out using MATLAB-Simulink. The comparison between these controllers is made considering the partial shading and their performance at different temperatures at the leading solar sites and South pole. Results indicate that there is an improvement in MPP tracking for both ANN and ANFIS controllers as compared to the P&O algorithm with respect to the settling time, overshoot, oscillations and time to achieve MPP at both environments.

Keywords: Maximum Power Point Tracking; Artificial Neural Network; Adaptive Neuro Fuzzy Inference System; Photovoltaic energy; Solar energy.

I. INTRODUCTION

Antarctic research facilities rely heavily on imported fuel oil, for their operations and safety measures to generate energy and provide heating and transportation services for both land and air activities in the area's environment. However, importation of fuel up to Antarctica and its delivery to the bases is expensive and its operations may pose risks since oil spills are a danger in any operations on the base [1]. For logistic reasons, as well as the remote location of the Antarctic bases, this also increases the cost of transporting fuel to areas that are not sea accessible [2]. Due to environmental considerations, it is necessary for the Antarctic bases to eliminate dependency on the fuel oil [3]. There are possibilities of harnessing wind and solar electricity in Antarctica, which can be a renewable energy alternative [4]. It does not matter what environmental issues exist; it is possible that renewable energy models would be cheaper than the current generation models [5].

The Amundsen-Scott South Pole Station, one of the research centers built by the United States at the geographical south pole is an example of why these alternatives are necessary. This institution, which has been managed since 1976 by the National Science Foundation (NSF), is one of the three USAP operated stations and is in the south pole with the other two being McMurdo Station on the Ross Sea, and Palmer Station on Anvers Island [6]. Built for the International Geophysical Year and establishing Upper Pole Station in November 1956, South Pole Station has been in operation for many years and in 1999, a modern elevated station was built [7]. Founded on the southwest polar cap at a height of 2835 m, the temperatures range between -13.6°C and -82.8°C with the station allowing extreme climatic conditions [8]. Such conditions require great specifics of engineering construction as well as a constant energy source to maintain the operability and even life [9]. Fig. 1 displays Amundsen-Scott South Pole Station [10].

[1] *Corresponding author: [1]Department of Electrical and Electronics Engineering, Istanbul Aydin University, Istanbul, Türkiye
[2] Department of Electrical and Electronics Engineering, Istanbul Aydin University, Istanbul, Türkiye

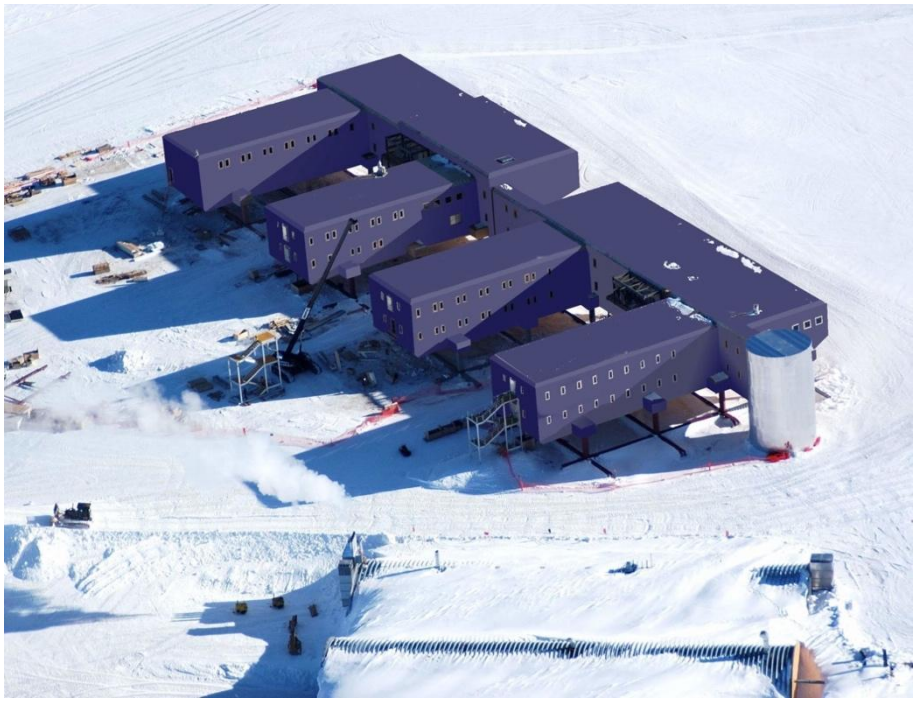

Fig. 1. Amundsen-Scott South Pole Station [10]

A. Green Energy Capability:

Among the researchers, the most renowned renewable technologies in Antarctica are wind and solar power and these have been widely used in applications [11]. Firstly, solar energy can be used for thermal applications or space heating and secondly, photovoltaic energy systems for the direct conversion of solar energy to electricity. The goal of this study is to investigate the effects of several methods for implementation of MPPT systems where conditions of the partial shadows and varying temperatures take place at the South pole and at other leading solar regions of the world.

B. South Pole Station's Atmospheric and Solar Statistics:

The National Aeronautics and Space Administration (NASA) furnishes satellite-derived surface meteorology and solar energy (SSE) data for any global coordinates [12]. This dataset provides a climate of solar irradiance and some meteorological data, for a period of ten years, on a grid of 1° by 1°. These means, however, may not completely characterize the localized microclimates but are relatively suited for the south pole applications.

At the South Pole, the following key points are observed:

Table 1 displays the average monthly insolation values which show the amount of solar energy received over a horizontal surface and measured in watt-hours in a single day [12].

Table 1. Monthly Averaged Insolation Incident (solar irradiation) On a Horizontal Surface (Wh/m^2/day) [12]

Latitude - 90^o Longitude 0^o	**Jan**	**Feb**	**Mar**	**Apr**	**May**	**June**	**July**	**Aug**	**Sep**	**Oct**	**Nov**	**Dec**
10-year average	864	467	46	0.00	0.00	0.00	0.00	0.00	0.09	296	734	964

Table 2 shows the average percentage of cloud amount at different hours in a day [12].

Table 2. Monthly Averaged Cloud Amount at Indicated GMT Times (%) [12]

Latitude -90º Longitude 0º	Jan	Feb	Mar	Apr	May	June	July	Aug	Sep	Oct	Nov	Dec
Average at 00:00	8.33	16.3	N/A	N/A	N/A	N/A	N/A	N/A	N/A	N/A	14.1	5.80
Average at 3:00	9.92	16.9	N/A	N/A	N/A	N/A	N/A	N/A	N/A	N/A	13.8	5.54
Average at 6:00	11.1	14.5	N/A	N/A	N/A	N/A	N/A	N/A	N/A	N/A	9.19	4.29
Average at 9:00	6.38	17.6	N/A	N/A	N/A	N/A	N/A	N/A	N/A	N/A	11.8	5.09
Average at 12:00	6.55	18.1	N/A	N/A	N/A	N/A	N/A	N/A	N/A	N/A	12.7	4.30
Average at 15:00	5.45	17.0	N/A	N/A	N/A	N/A	N/A	N/A	N/A	N/A	10.9	5.21
Average at 18:00	6.74	15.8	N/A	N/A	N/A	N/A	N/A	N/A	N/A	N/A	11.2	4.97
Average at 21:00	7.49	16.9	N/A	N/A	N/A	N/A	N/A	N/A	N/A	N/A	15.1	6.34

Table 3 displays the data of monthly averaged wind speed measured 50 meters above the Earth surface [12].

Table 3. Monthly Averaged Wind Speed at 50 m Above the Surface of The Earth (m/s) [12]

Latitude -90º Longitude 0º	Jan	Feb	Mar	Apr	May	June	July	Aug	Sep	Oct	Nov	Dec
10-year average	4.63	5.59	7.02	7.33	7.35	7.31	7.16	7.25	7.24	6.30	4.91	4.15

Table 4 displays the minimum and maximum difference of monthly averaged wind speed measured 50 meters above the Earth surface [12].

Table 4. Minimum And Maximum Difference from Monthly Averaged Wind Speed at 50 m (%) [12]

Latitude -90º Longitude 0º	Jan	Feb	Mar	Apr	May	June	July	Aug	Sep	Oct	Nov	Dec
Minimum	-8	-10	-11	-8	-7	-6	-4	-5	-6	-5	-11	-17
Maximum	8	9	5	5	5	6	7	2	7	5	13	19

Table 5 shows monthly averaged temperature measured at 10 meters above the Earth surface at different intervals in a day [12].

Table 5. Monthly Averaged Air Temperature At 10 m Above the Surface of The Earth for Indicated GMT Times (° C) [12]

Latitude -90º Longitude 0º	Jan	Feb	Mar	Apr	May	June	July	Aug	Sep	Oct	Nov	Dec
Average at 22:30	-21.4	-29.7	-46.8	-55.9	-58.1	-59.3	-61.3	-64.1	-63.2	-52.1	-30.1	-21.4
Average at 01:30	-21.5	-29.9	-47.2	-55.9	-58.1	-59.3	-61.3	-64.0	-63.2	-52.2	-30.1	-21.4
Average at 04:30	-21.6	-30.1	-47.7	-55.9	-58.1	-59.4	-61.3	-64.0	-63.2	-52.4	-30.2	-21.5
Average at 07:30	-21.7	-30.2	-47.7	-56.0	-58.1	-59.5	-61.3	-63.9	-63.2	-52.3	-30.2	-21.5
Average at 10:30	-21.6	-30.2	-47.8	-56.1	-58.2	-59.5	-61.3	-63.9	-63.2	-52.0	-30.0	-21.5
Average at 13:30	-21.6	-30.1	-47.6	-56.3	-58.2	-59.5	-61.4	-63.9	-63.2	-52.7	-30.7	-21.3
Average at 16:30	-21.5	-30.0	-47.2	-56.2	-58.2	-59.5	-61.4	-63.9	-63.1	-52.4	-30.6	-21.3
Average at 19:30	-21.5	-30.0	-47.0	-56.1	-58.2	-59.4	-61.5	-63.9	-63.1	-52.4	-30.6	-21.2

It is evident that during the summer months there is a great deal of solar energy that can be harnessed due to increased solar radiation and less cloud coverage. In addition, photovoltaic cells richer in silicon also have a better performance in cooler environments. For silicon cells, their power output is greatest at low temperatures, approximately - 0.4% per degree Centigrade. These are less on the South Pole where the wind velocities are not very high, hence, the structural stresses on the solar panel installations are further reduced.

C. Comparison with Leading Solar Sites:

For a more tangible estimation of what the South Pole can achieve, its solar outputs can be put side by side with some of the leading photovoltaic sites. For example, the 11 MW solar plant in Serpa, Portugal, and an 8 MW installation to be in Colorado's San Luis Valley are some examples of large-scale solar projects. In this study, we benchmarked these sites against the South Pole by utilizing NASA's SSE data.

1. Serpa, Portugal

Table 6 shows the average monthly insolation values which show the amount of solar energy received over a horizontal surface and measured in watt-hours in a single day in Serpa, Portugal [12] which is one of the leading solar sites.

Table 6. Monthly Averaged Insolation Incident on A Horizontal Surface (Wh/m^2/day) [12]

Serpa	Jan	Feb	Mar	Apr	May	June	July	Aug	Sep	Oct	Nov	Dec
10-year average	231	300	436	520	615	688	734	650	521	351	241	194

2. San Luis Valley, Colorado

Table 7 displays the average monthly insolation values which show the amount of solar energy received over a horizontal surface and measured in watt-hours in a single day in San Luis Valley, Colorado [12].

Table 7. Monthly Averaged Insolation Incident on A Horizontal Surface (Wh/m^2/day) [12]

San Luis	Jan	Feb	Mar	Apr	May	June	July	Aug	Sep	Oct	Nov	Dec
10-year average	235	326	441	552	640	655	603	539	480	381	273	218

Fig. 2 displays the comparison of solar irradiation between South Pole and leading solar sites [12].

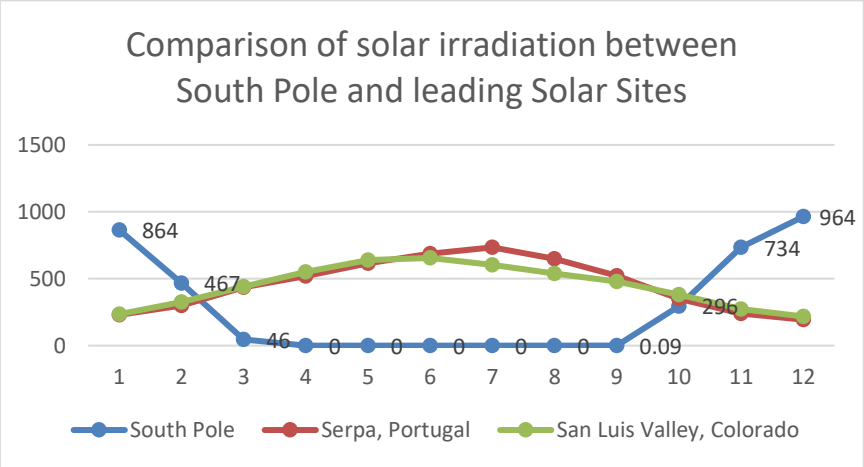

Fig. 2. Average insolation vs month for the South Pole, Serpa (Portugal) and the San Luis Valley (Colorado, USA)

Given that the annual mean solar energy at the South Pole is approximately 60% of the best current solar energy sites worldwide, efficiency improvements at low temperatures and constant summer solar irradiation raise the South Pole to one of the leading candidates for implementing renewable energy [13].

II. Maximum Power Point Tracking (MPPT)

Solar energy technology today provides about 16% of global energy consumption [14] – [16], apart from being a clean energy solution due to its low operational costs. With more efficiency than other renewable sources, PV turned out to be one of the safest and most capable sources of energy [17]. Nevertheless, photovoltaic systems are faced with another challenge-its low efficiency [18].

The output characteristics of PV arrays are non-linear and dependent on atmospheric conditions: sunlight intensity and temperature shown in Fig. 3. This causes the MPP to be different for different conditions. To achieve maximum energy production, PV systems should be operated at maximum power point always. Various Maximum Power Point Tracking (MPPT) controllers have been developed throughout the years regarding solar PV, to achieve that aim. These controllers essentially handle the duty cycle of DC-DC converters to produce maximum output power at the MPP. MPP, denoted by(V_{mp}, I_{mp}), can be interpreted in few words, "both voltage and current intersect". The MPP methods increase the efficiency of systems and lower the total costs of PV installations.

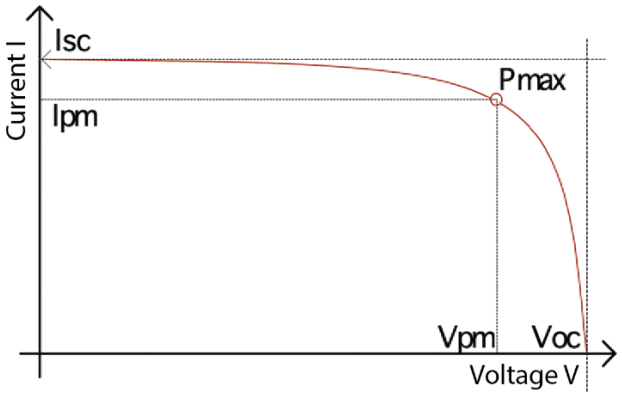

Fig. 3. Output characteristics of PV cell

Different MPPT algorithms have been introduced in different levels of complexity, accuracy, operational cost, and sensor requirements [19]. The Perturb and Observe (P&O) method is the most widely used mainly because of its simplicity. Rapid changes in solar irradiation make a MPP not stable, and steady-state oscillations pose a common disadvantage [20]. For fast and stable responses compared to conventional algorithms, more sophisticated approaches like fuzzy logics and ANNs have demonstrated substantial success in the MPP tracking process [21] ,[22].

The ANN-based MPPT controllers have an upper hand in adjusting various non-linear characteristics of PV modules with respect to environmental uncertainties. These controllers use diverse algorithms with, respectively, defined input and output variables and specified sensor requirements [23] – [27]. Adaptive Neuro-Fuzzy Inference Systems (ANFIS) can additionally improve efficiency to settle relatively faster, with lesser overshoot and oscillation, whilst tracking the MPP with far more effectiveness compared to ANN based methods.

A. Perturb and Observe (P & O) MPPT:

The Perturb and Observe (P&O) method is a traditional MPPT algorithm that works by perturbing the operating voltage and observing the resulting changes in power. If the power increases, the algorithm continues in the same direction; otherwise, it reverses direction. While it is simple and widely used, the P&O method may struggle with dynamic environmental changes and can oscillate around the maximum power point.

The P&O method is very well known for being easy to implement [28]. It modifies the duty cycle of the DC-DC converter dependent upon the sampled voltage at the PV module to arrive at the optimal operating point. A flowchart of the P&O algorithm is presented in Fig. 4. If the next perturbation increases power output, this perturbation is in the same direction as the previous one. Otherwise, the perturbation is reversed in order to approach the MPP [29].

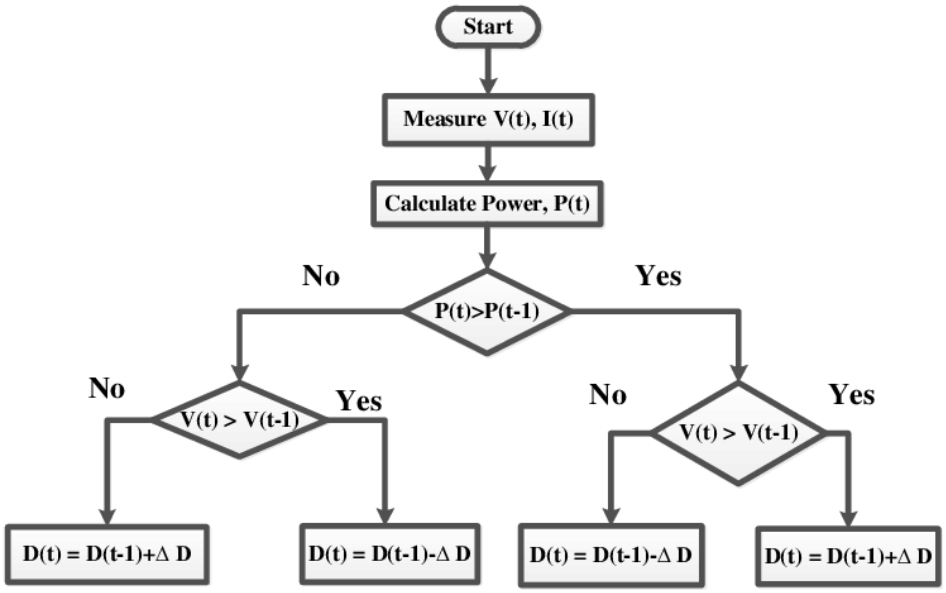

Fig. 4. P&O algorithm's flow chart

Although modified adaptive P&O algorithms do successfully mitigate some limitations of the traditional approach, challenges of oscillation very near the MPP and difficulties of tracking under rapidly changing conditions do persist.

B. Artificial Neural Network (ANN) MPPT:

Artificial Neural Network (ANN) based MPPT take historical data such as solar irradiance and temperature, in addition to real-time inputs to be able to predict the maximum power operating point efficiently. The advantages of ANN are that it can learn to adapt itself to a changing operating environment. It is significantly faster and more accurate than ordinary algorithms in terms of bringing in the required results.

An artificial neural network imitates the connected neurons found in the human brain whereby communication is enabled through adjustable-weight connections. Fig. 5 elaborates on the architecture of a general ANN.

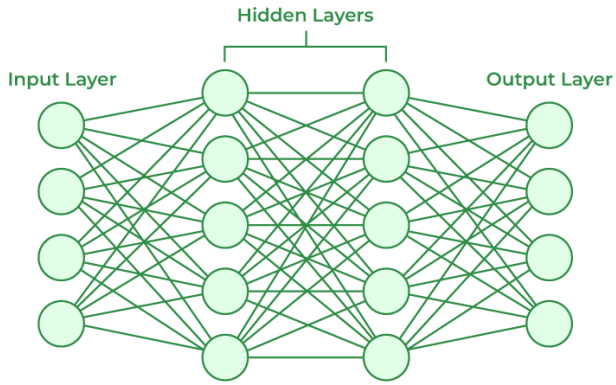

Fig. 5. Architecture Artificial Neural Network's Architecture

Weights indicate the importance of each input and training generally involves a dedicated adjustment of these weights. During the training of ANN, the inputs (features) and outputs (targets) are compared, and in case of mismatches, the error is reduced through repeated iterations [30]. For MPPT applications, ANN algorithms use irradiance and temperature sensors found to be useful in acquiring the best duty cycle for converter operation [31]. Other systems additionally incorporate various sensors to track the voltage and current, thereby assuring the accuracy in tracking the MPP [23] , [32].

The ANN modeled in this study consists of an input layer, a hidden layer, and an output layer. A tangent sigmoid activation function is employed on the hidden layer, while the output layer uses a linear transfer function. The performance of the neural network is assessed through mean square error (MSE), given by:

$$E_{\text{mse}} = \sum_{k=1}^{N} [\, t(k) - o(k)]^2 \qquad (1)$$

where t(k) is the target at sample k, o(k) is the output at sample k, and N is the number of total training patterns.

This study finds the MPPT process divided into two different stages: MATLAB trains the ANN in determining the optimal voltages points (V_{pv}) that refer to the power points under tracking; controller PI adjusts the duty cycle on the converter for the MPP. This is depicted in Fig. 6 of the ANN-based MPPT algorithm.

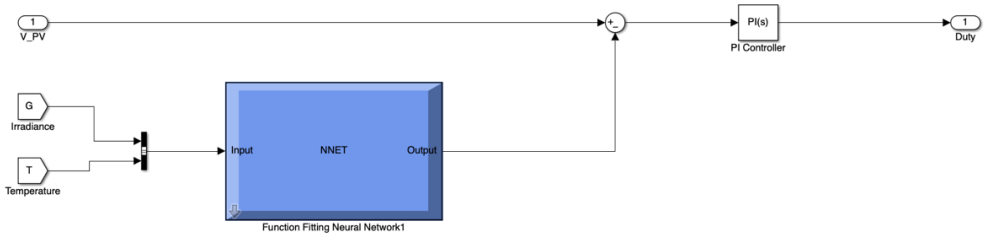

Fig. 6. Simulink model for ANN method

C. Adaptive Neuro Fuzzy Inference System (ANFIS) MPPT:

Adaptive Neuro-Fuzzy Inference System (ANFIS) is the combination of the two methods — fuzzy logic and neural networks, building a self-learning system even in the presence of uncertainties and nonlinearities. It offers a very robust and intelligent approach to MPPT for complicated or dynamically changing scenarios.

Adaptive Neuro-Fuzzy Inference System (ANFIS), a combination of neural networks and fuzzy logic in the analysis of nonlinear characteristics of PV systems, utilizes current (Ipv) and voltage (Vpv) as inputs and forms duty cycle (α) as output [33] , [34].

Extensive prior datasets were utilized as knowledge to train the ANFIS controller [33]. Each input has five triangular membership functions, and fuzzy If-then rules are refined to improve results. The controller during training organizes membership functions to give good performance by minimizing errors. Upon finishing the training process, the controller validates the data to ensure optimum operation [35].

It is quite well recognized that ANFIS controllers are distinguished by their accuracy, flexibility, convergence speeds, and near-zero oscillation despite different environmental conditions. Fig. 7 illustrates the implementation of ANFIS-based MPPT:

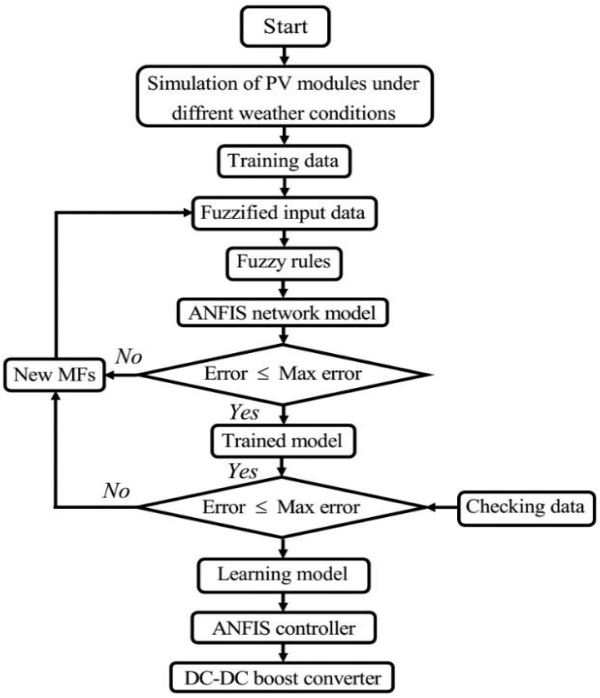

Fig. 7. ANFIS based MPPT implementation flowchart

III. MATERIAL AND METHODS

A. Simulation of PV Module:

The PV module "**SunPower SPR-E20-440-COM"** is simulated in this study. Table 8 shows the data sheet for the reference model under standard test conditions (STC).

Table 8. Specification of the PV module

Parameter	Value
Maximum power (P_{max})	444.86 W
Maximum power voltage (V_{mp})	76.7 V
Maximum power current (I_{mp})	5.8 A
Open circuit voltage (V_{oc})	90.5
Short circuit current (I_{sc})	6.21 A
Maximum system voltage	383.5 V
Standard test condition (STC)	Cell temperature: 25^{O}C, irradiance: 1000 W/m^2

This project involves the design of a 3 MW PV array. It comprises 5 modules in series per string and 1,349 parallel strings. The voltage-power (V-P) and voltage-current (V-I) characteristics of the module are shown in Fig.s 8 and 9. From these simulation results, it can be noted how the MPP varies and moves with solar irradiation

and temperature.

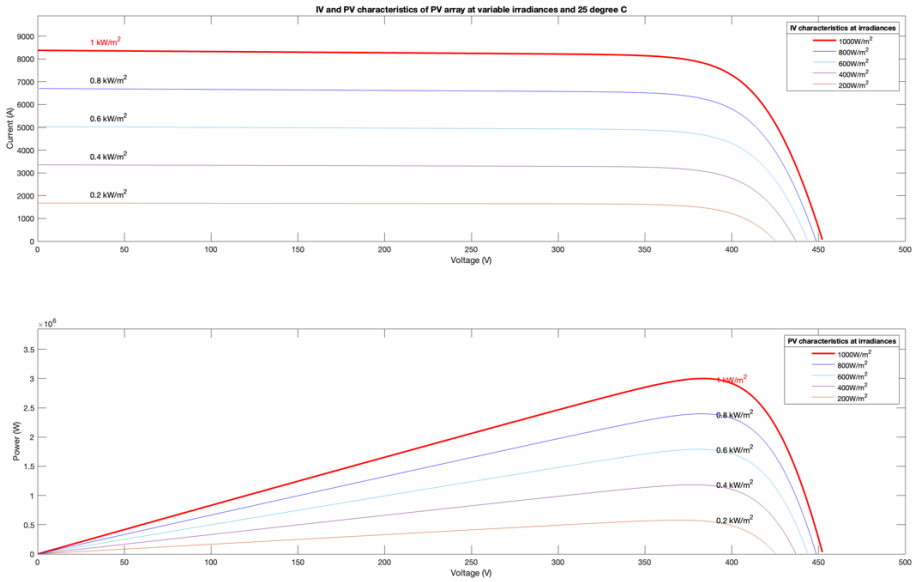

Fig. 8. V-I and V-P characteristics of the PV module and location of the MPP for different irradiations at 25°C

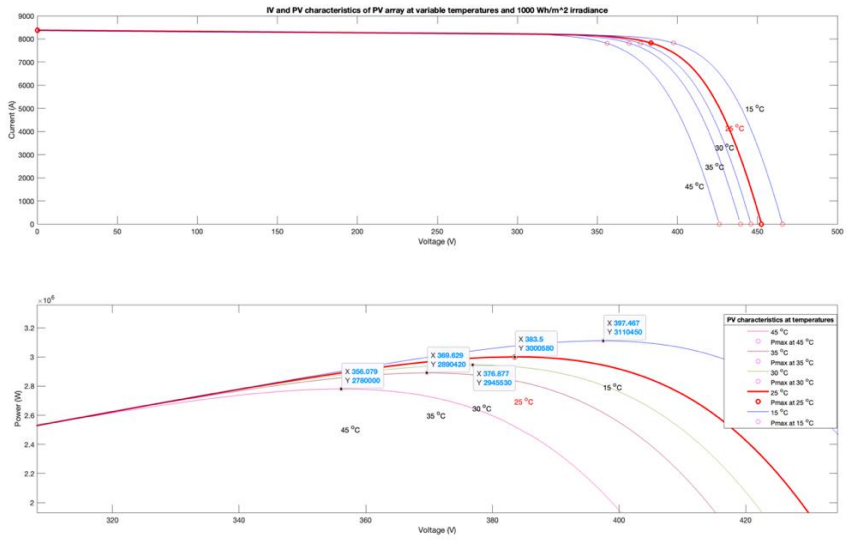

Fig. 9. V-I and V-P characteristics of the PV module and location of the MPP for different temperatures at 1000W/h

B. **DC-DC Boost Converter:**

The DC-DC boost converter is used for connecting the PV array to the load, for maximum power extraction under different environmental and load conditions. Fig. 10 displays the structure of DC-DC Boost converter:

- Input voltage source (PV array)
- Output voltage load
- A Switching component: MOSFET or IGBT in parallel with a diode
- A Filter for output current: inductor (L)
- A Smoothing output voltage: capacitor (Co)

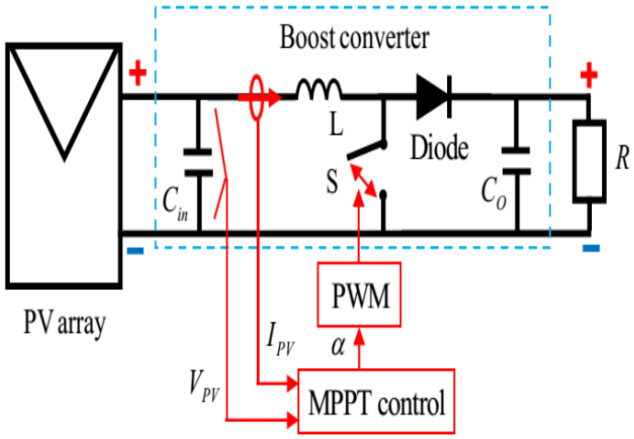

Fig. 10. General Structure of DC-DC Boost Converter

C. **MPPT Controllers:**

1. **Perturb and Observe (P&O) based MPPT controller:**

The Perturb and Observe (P&O) MPPT controller in Fig. 11, allows the solar irradiation levels to change rapidly between 1000 W/m^2 and 400 W/m^2 showing partial shading effect. Temperature ranges are varied from 15-degree centigrade to 45-degree centigrade for typical solar sites and from -55 degrees centigrade to -20 degrees centigrade for the South Pole.

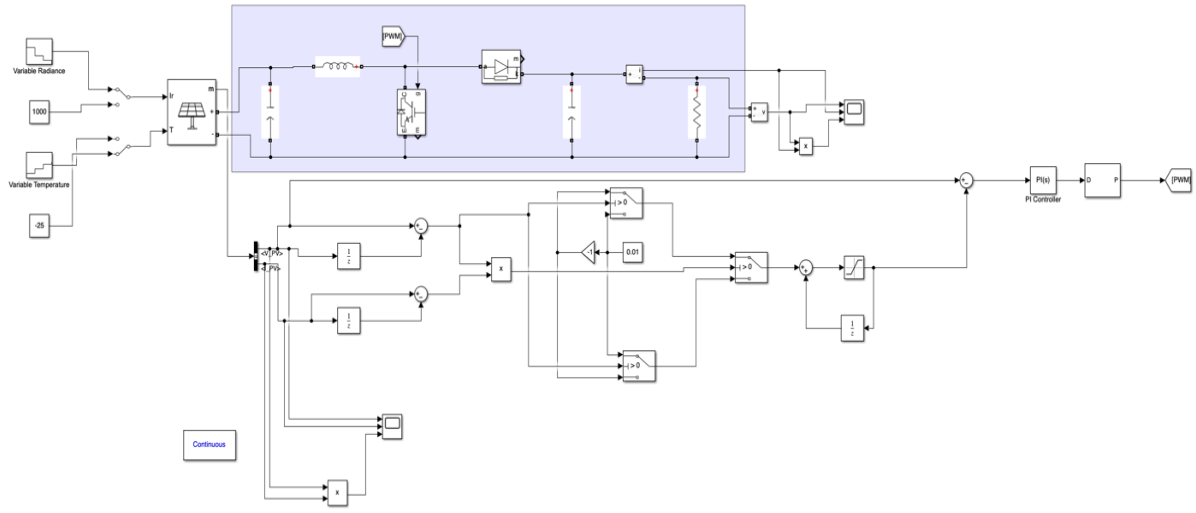

Fig. 11. Perturb and observe based MPPT controller

2. Artificial Neural Network (ANN) based MPPT controller:

The Fig. 12 shows the ANN-controlled MPPT. The output from PV array gets compared against the predictions by the neural network model. The resulting difference is solved using the proportional-integrative (PI) controller that modifies the duty cycle of the IGBT switch to reach maximum power output. The neural network algorithm employed is shown in Fig. 13.

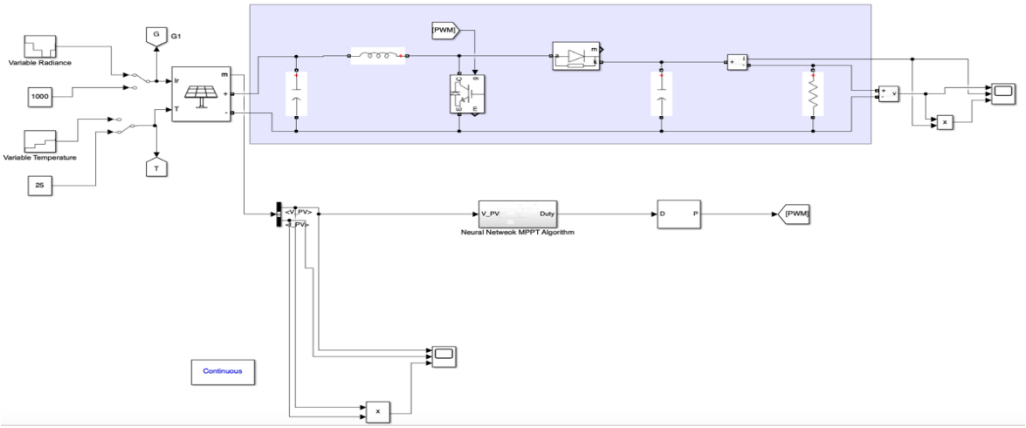

Fig. 12. Artificial Neural Network (ANN) based MPPT controller

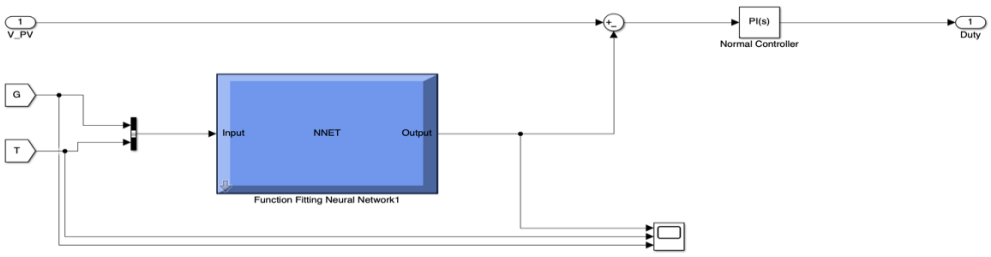

Fig. 13. Neural Network algorithm

3. Adaptive Neuro Fuzzy Inference System (ANFIS) based MPPT controller:

The ANFIS-controlled MPPT seen in Fig. 14 uses fuzzy logic for voltage estimation. This voltage error signal is forwarded to a PI controller that computes the required duty cycle to be applied to the IGBT switch. The ANFIS algorithm is presented in detail in Fig. 15 and 16 together with its structure.

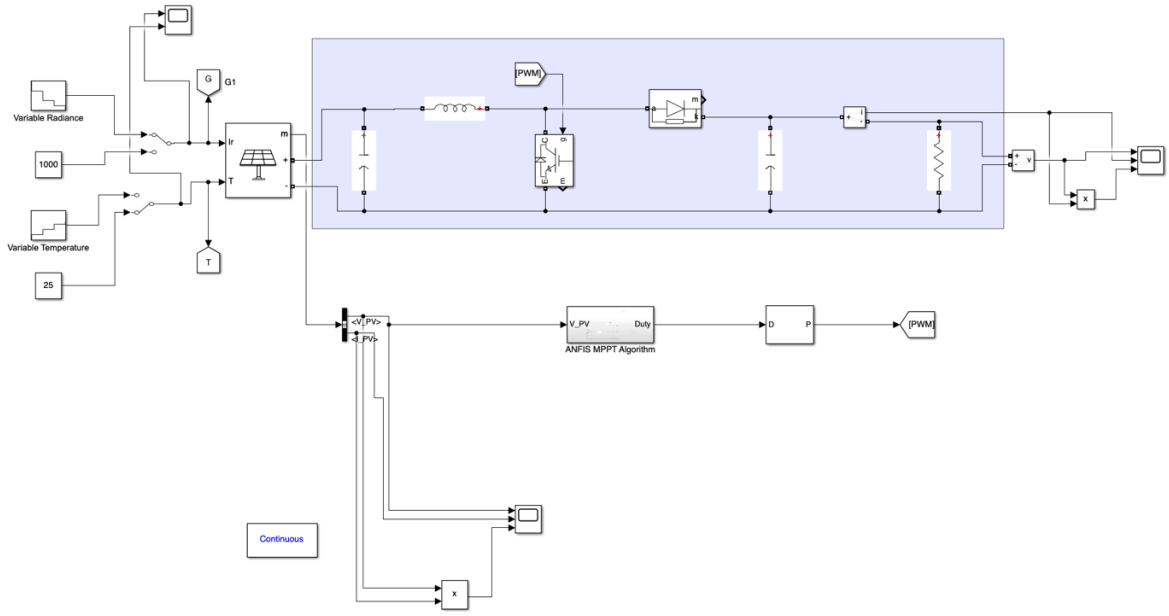

Fig. 14. ANFIS based MPPT controller

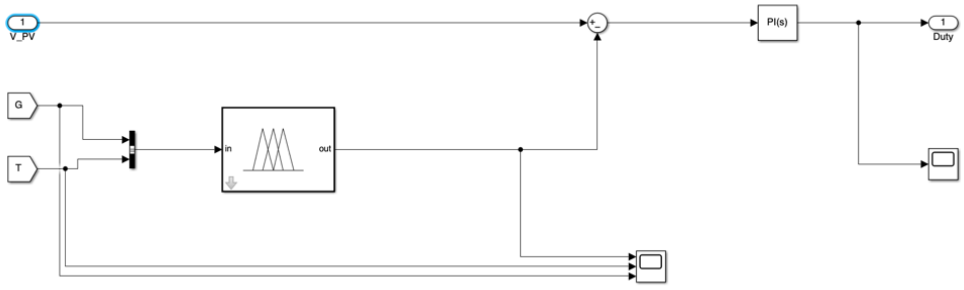

Fig. 15. ANFIS block algorithm

Structure for ANFIS is shown in Fig. 16.

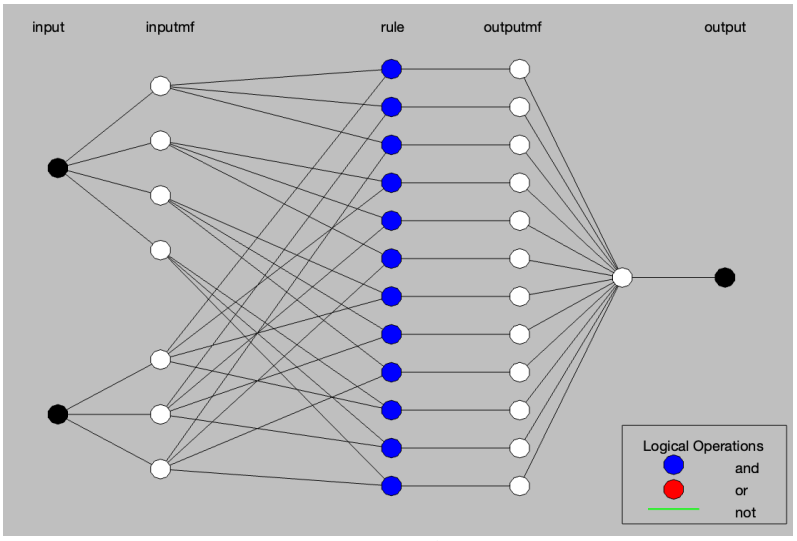

Fig. 16. Structure for ANFIS

IV. RESULTS AND DISCUSSION

PV array is designed to provide the maximum power of 3MW at 1000 W/m^2 irradiance and 25ºC temperature. In South Pole due to lower temperature values (-55ºC to -20ºC) PV array is supposed to give power more than 3MW as solar cells perform better at low temperatures. Partial shading effect is applied by changing the solar irradiation abruptly between values of 1000 W/m^2 to 400 W/m^2 by keeping the temperature constant at 25ºC for leading solar sites and -25ºC for South Pole. For evaluating the performance of controller in leading solar sites temperature is varied in steps from 15ºC to 45ºC while for South Pole the temperature is varied from -55ºC to -20ºC. Solar irradiation is kept constant at 1000W/m^2 at both locations for this. Performance of each technique based MPPT controller is given below.

A. Performance of P&O based MPPT Controller:

Fig. 17 and 18 show the performance of P&O based controller at leading solar sites with varying solar irradiation abruptly (for partial shading effect) and variable temperatures respectively.

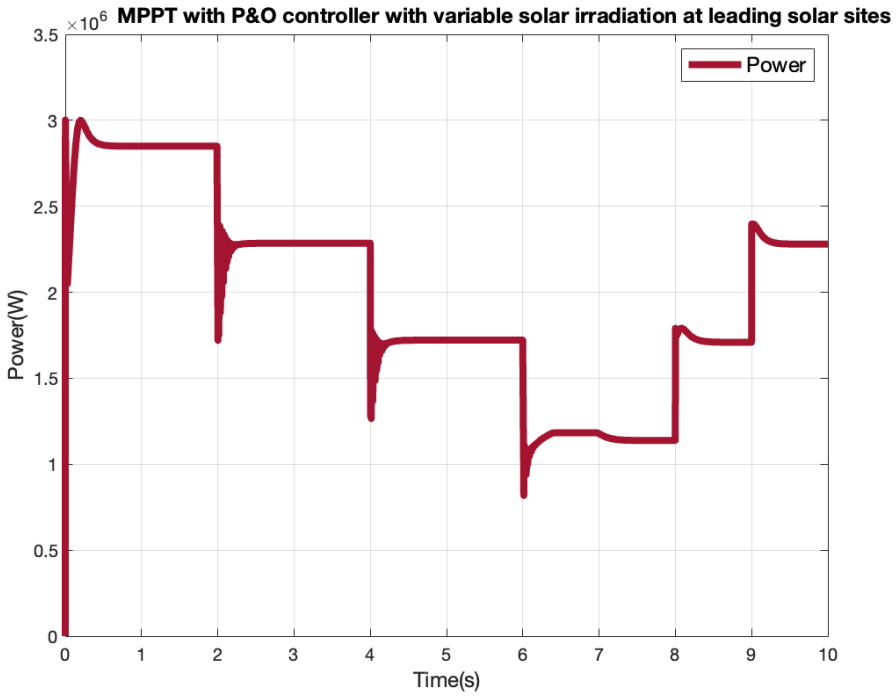

Fig. 17. MPPT with P&O based controller with variable solar irradiation at leading solar sites

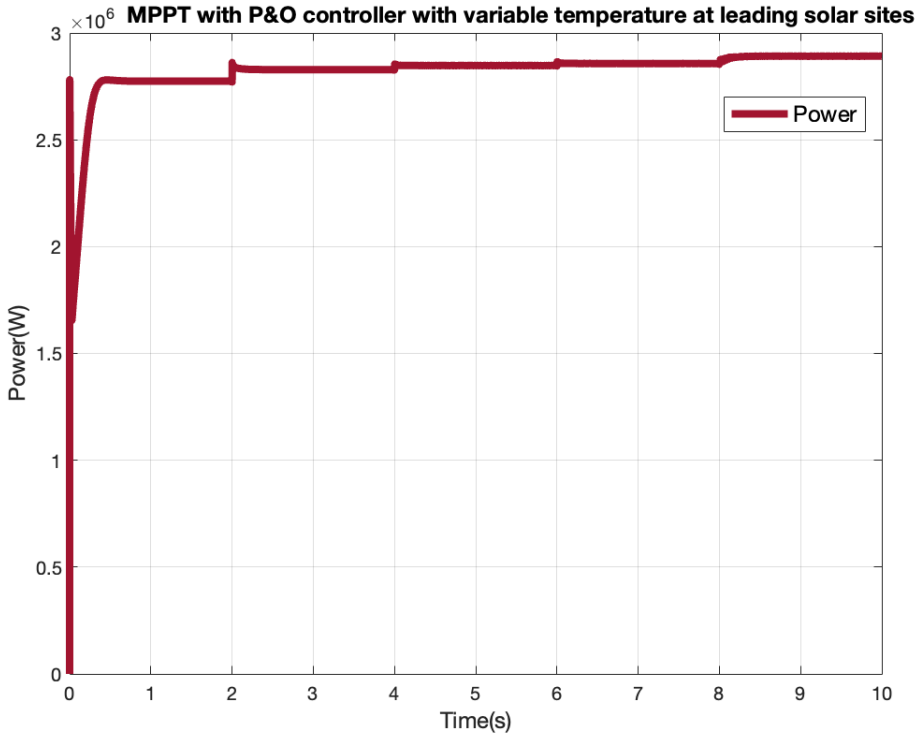

Fig. 18. MPPT with P&O based controller with variable temperature at leading solar sites

Similarly, the performance of P&O based controller at South pole with varying solar irradiation abruptly (for partial shading effect) and variable temperatures are shown in Fig. 19 and 20 respectively.

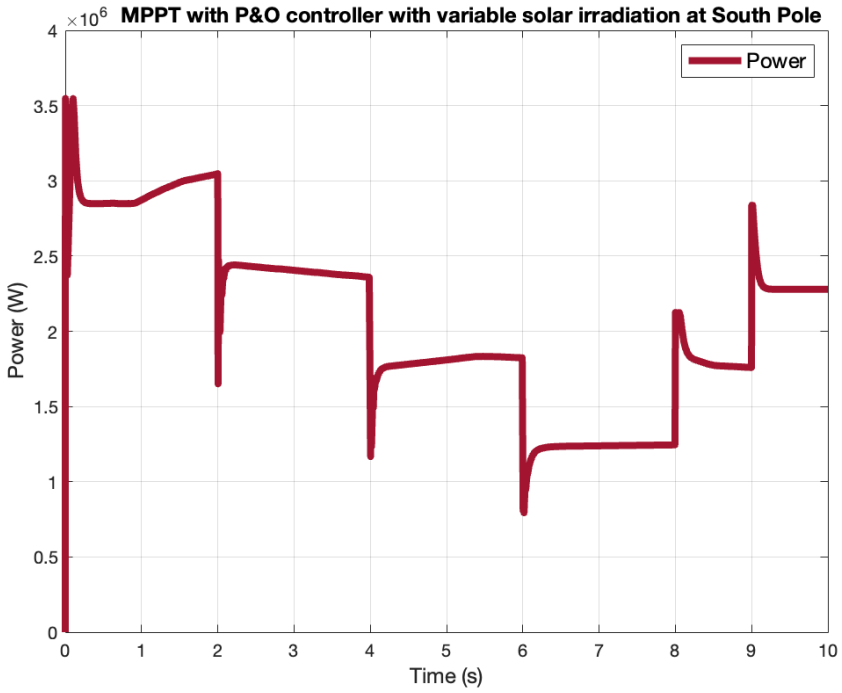

Fig. 19. MPPT with P&O based controller with variable solar irradiation at South Pole

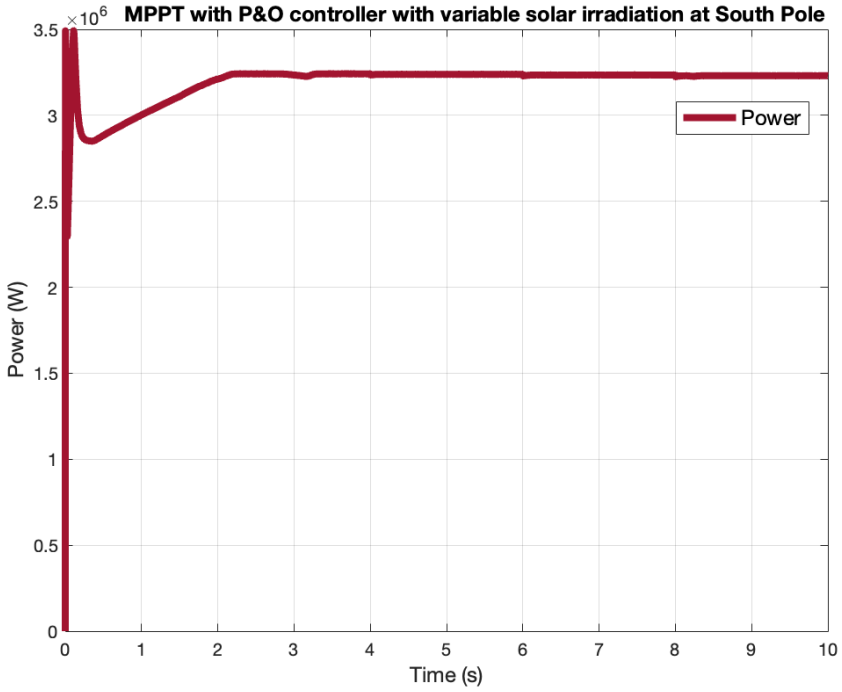

Fig. 20. MPPT with P&O based controller with variable temperature at South Pole

These results can be shown in the form of tables for easy evaluation. Table 9 and 10 summarize the performance of P&O based MPPT controller with varying irradiance and varying temperature both at leading solar sites and South Pole respectively.

Table 9. Power obtained by P&O based MPPT controller with varying irradiance

Location	1000 W/m^2	800 W/m^2	600 W/m^2	400 W/m^2	600 W/m^2	800 W/m^2
Leading Solar Site	2.8498 MW	2.2849 MW	1.7216 MW	1.1387 MW	1.7097 MW	2.2800 MW
South Pole	3.0175 MW	2.3749 MW	1.8308 MW	1.2420 MW	1.7658 MW	2.2784 MW

The upper temperature in table below is for leading solar sites and lower is for South Pole.

Table 10. Power obtained by P&O based MPPT controller with varying temperature

Location	45ºC -20 ºC	35 ºC -25 ºC	30 ºC -35 ºC	25 ºC -45 ºC	15 ºC -55 ºC
Leading Solar Site	2.7740 MW	2.8284 MW	2.8472 MW	2.8571 MW	2.8916 MW
South Pole	3.1762 MW	3.2408 MW	3.2380 MW	3.2348 MW	3.2297 MW

It is clear from results that P&O based MPPT controller fails to obtain the rated 3MW power at leading solar sites. At South Pole the power obtained for each irradiation is more than that obtained at leading solar sites which is due to lower temperatures but still we can conclude that it fails to get the maximum power at South Pole too. Varying temperature has drastic effect on P&O based MPPT controller at South Pole as it fails to provide constant power even if the temperature is kept constant for a period. With partial shading effect, it fails to get the same power it gets for the same irradiance before.

B. **Performance of ANN based MPPT Controller:**

Fig. 21 and 22 show the performance of ANN based controller at leading solar sites with varying solar irradiation abruptly (for partial shading effect) and variable temperatures respectively.

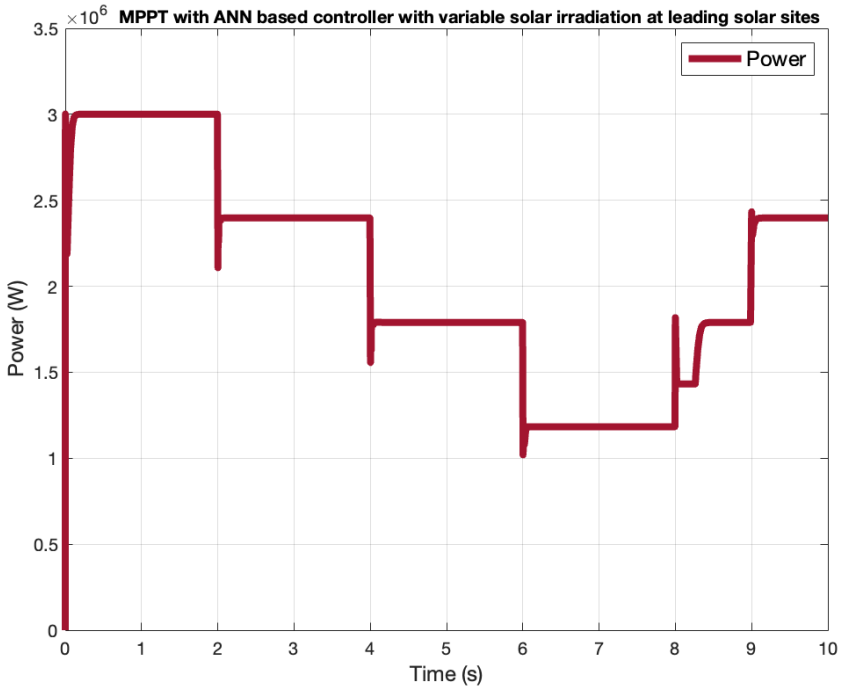

Fig. 21. MPPT with ANN based controller with variable solar irradiation at leading solar sites

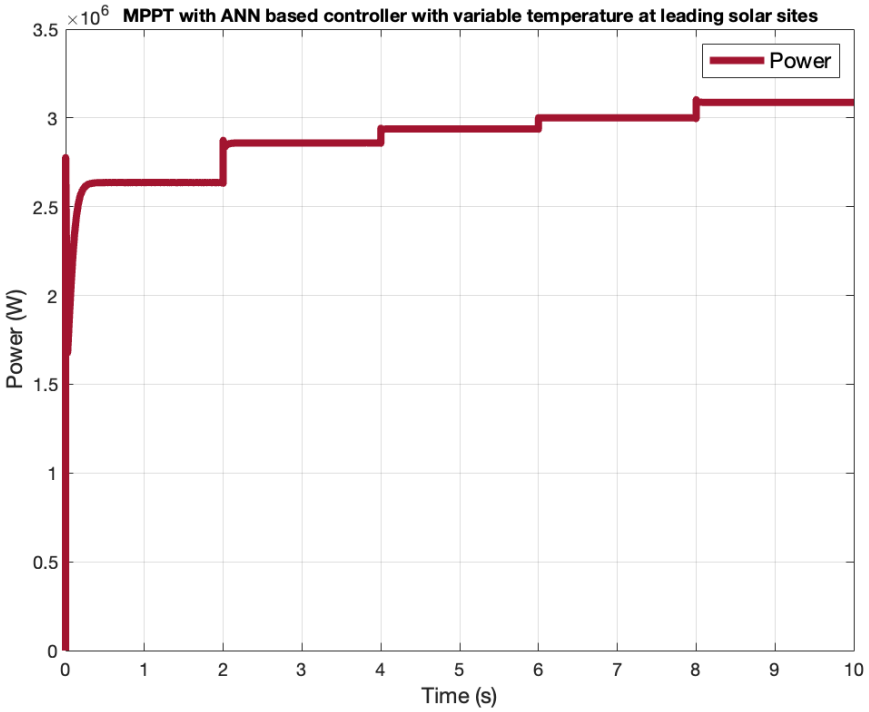

Fig. 22. MPPT with ANN based controller with variable temperature at leading solar sites

Similarly, the performance of ANN based controller at South pole with varying solar irradiation abruptly (for partial shading effect) and variable temperatures are shown in Fig. 23 and 24 respectively.

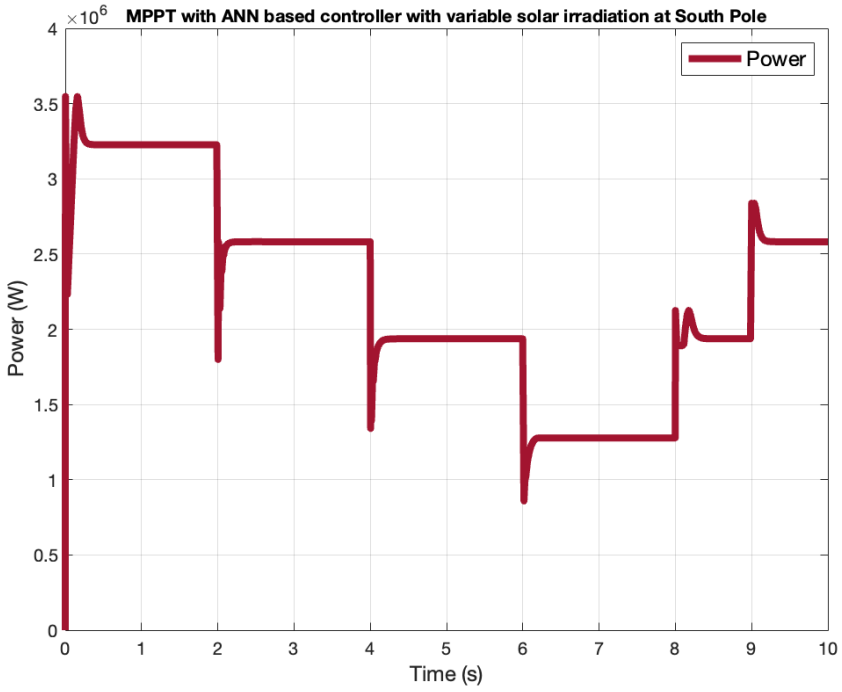

Fig. 23. MPPT with ANN based controller with variable solar irradiation at South Pole

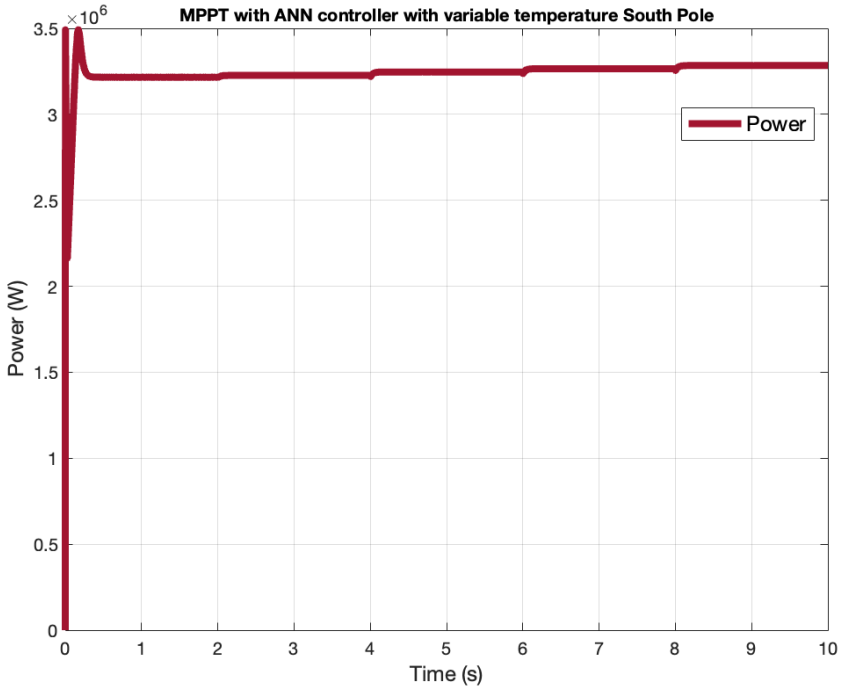

Fig. 24. MPPT with ANN based controller with variable temperature at South Pole

These results can be shown in the form of tables for easy evaluation. Table 11 and 12 summarize the performance of ANN based MPPT controller with varying irradiance and varying temperature both at leading solar sites and South Pole respectively.

Table 11. Power obtained by ANN based MPPT controller with varying irradiance

Location	1000 W/m^2	800 W/m^2	600 W/m^2	400 W/m^2	600 W/m^2	800 W/m^2
Leading Solar Site	3 MW	2.3973 MW	1.7899 MW	1.1828 MW	1.7899 MW	2.3973 MW
South Pole	3.2265MW	2.5816 MW	1.9366 MW	1.2766 MW	1.9365 MW	2.5815 MW

The upper temperature in table below is for leading solar sites and lower is for South Pole.

Table 12. Power obtained by ANN based MPPT controller with varying temperature

Location	45ºC -20 ºC	35 ºC -25 ºC	30 ºC -35 ºC	25 ºC -45 ºC	15 ºC -55 ºC
Leading Solar Site	2.6357 MW	2.8593 MW	2.9383 MW	3 MW	3.0875 MW
South Pole	3.2156 MW	3.2264 MW	3.2464 MW	3.2652 MW	3.2835 MW

Artificial Neural Network (ANN) based MPPT controller is clearly performing better than P&O based MPPT controller in obtaining maximum power from the PV array both at leading solar sites and South Pole. It attains steady state more rapidly than P&O based controller and partial shading also has minimum effect as same power is obtained for same value of irradiation.

C. **Performance of ANFIS based MPPT controller:**

Fig. 25 and 26 show the performance of ANFIS based controller at leading solar sites with varying solar irradiation abruptly (for partial shading effect) and variable temperatures respectively.

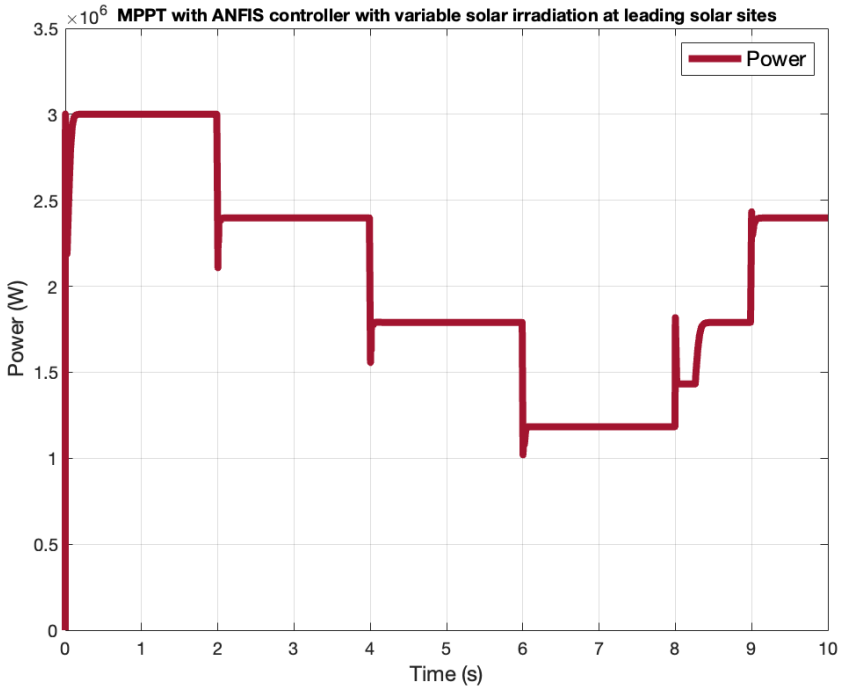

Fig. 25. MPPT with ANFIS based controller with variable solar irradiation at leading solar sites

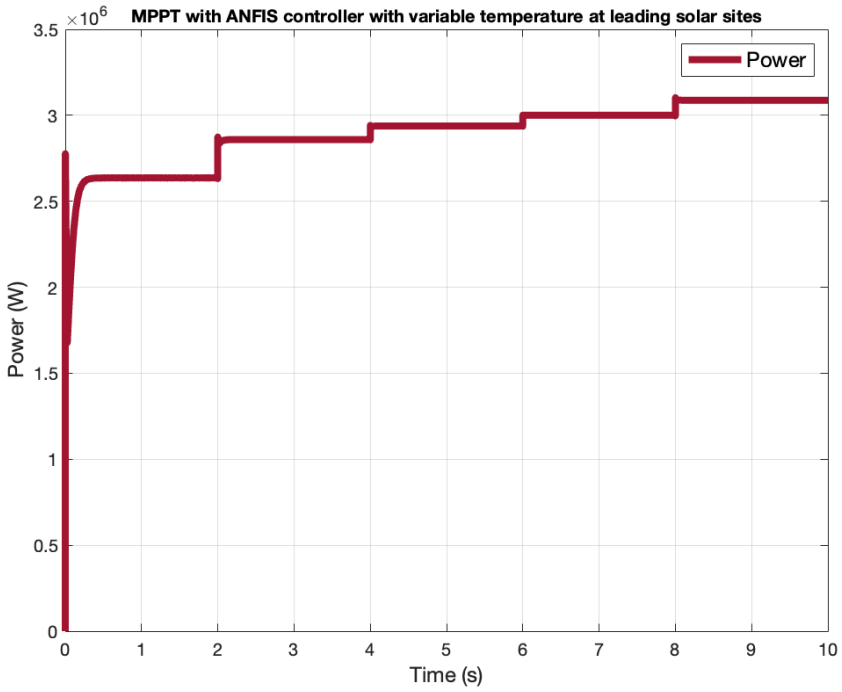

Fig. 26. MPPT with ANFIS based controller with variable temperature at leading solar sites

Similarly, the performance of ANN based controller at South pole with varying solar irradiation abruptly (for partial shading effect) and variable temperatures are shown in Fig. 27 and 28 respectively.

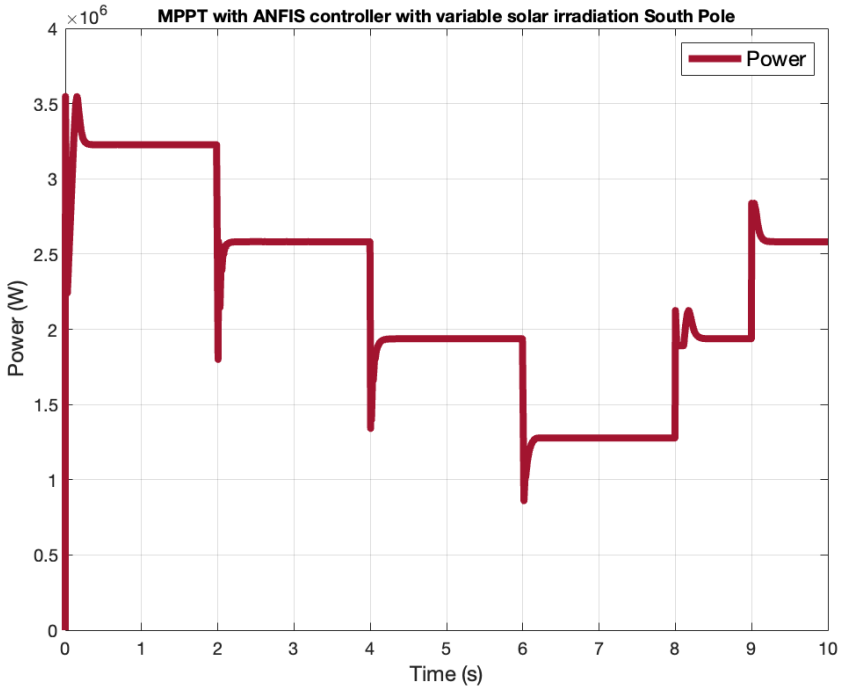

Fig. 27. MPPT with ANFIS based controller with variable solar irradiation South Pole

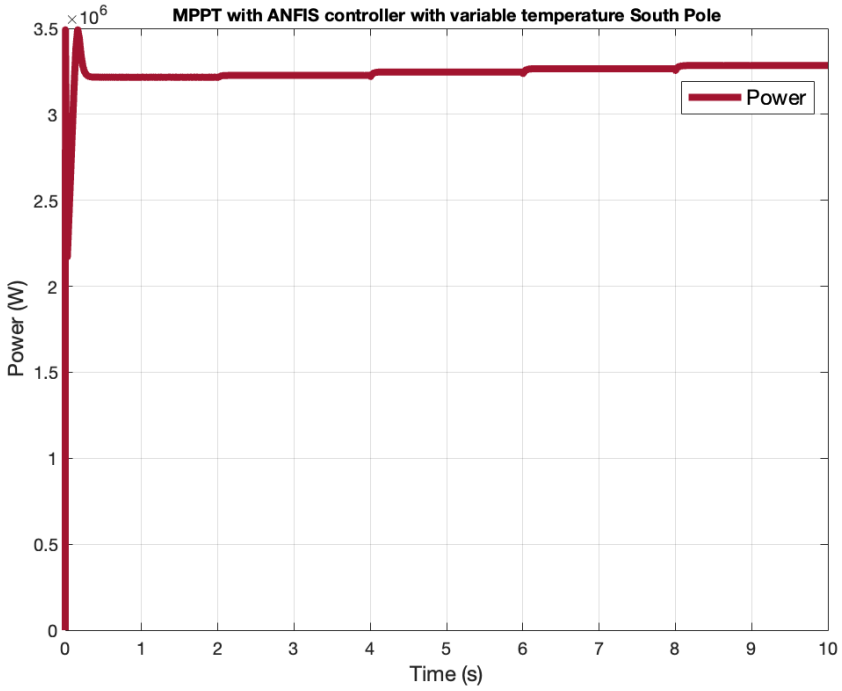

Fig. 28. MPPT with ANFIS based controller with variable temperature at South Pole

These results can be shown in the form of tables for easy evaluation. Table 13 and 14 summarize the performance of ANN based MPPT controller with varying irradiance and varying temperature both at leading solar sites and South Pole respectively.

Table 13. Power obtained by ANFIS based MPPT controller with varying irradiance

Location	1000 W/m^2	800 W/m^2	600 W/m^2	400 W/m^2	600 W/m^2	800 W/m^2
Leading Solar Site	3 MW	2.3974 MW	1.7899 MW	1.1828 MW	1.7899 MW	2.3973 MW
South Pole	3.226 MW	2.582 MW	1.937 MW	1.277 MW	1.937 MW	2.582 MW

The upper temperature in table below is for leading solar sites and lower is for South Pole.

Table 14. Power obtained by ANFIS based MPPT controller with varying temperature

Location	45ºC -20 ºC	35 ºC -25 ºC	30 ºC -35 ºC	25 ºC -45 ºC	15 ºC -55 ºC
Leading Solar Site	2.636 MW	2.8591 MW	2.9383 MW	3 MW	3.0876 MW
South Pole	3.2156 MW	3.2265 MW	3.2463 MW	3.2653 MW	3.2835 MW

The results obtained from ANFIS based MPPT controller are very much like those obtained from ANN based MPPT controller. Both attain steady state more rapidly than P&O based controller and partial shading also has minimum effect as same power is obtained for same value of irradiation.

V. CONCLUSION

This paper evaluates the performance of Perturb and Observe (P&O) based MPPT techniques with Artificial Neural Network (ANN) and Adaptive Neuro-Fuzzy Inference System (ANFIS) based MPPT techniques in leading solar sites and South Pole. In the presence of rapidly changing sun irradiation or temperature, the ANN and ANFIS algorithms are extremely fast and precise in locating and monitoring the MPP at both locations. On the contrary, when irradiation changes rapidly in a short period of time, the P&O approach fails to detect the MPP. Furthermore, this approach exhibits substantial oscillation around MPP resulting in significant power loss over time.

Declaration of Ethical Standards

The authors declare that this study complies with ethical standards and does not involve any human participants or animals.

Declaration of Competing Interest

The authors declare that they have no competing financial or personal interests that could have influenced the work reported in this paper.

Funding / Acknowledgements

No funding was received for this study.

REFERENCES

[1] T. Tin, B. K. Sovacool, D. Blake, P. Magill, S. El Naggar, S. Lidstrom, and M. Ishizawa, “Energy efficiency and renewable energy under extreme conditions: Case studies from Antarctica,” Renew. Energy, vol. 35, no. 8, pp. 1715–1723, Aug. 2010.
[2] A. D. Hemmings, “Why fuel matters: Energy needs in Antarctic systems,” Polar Rec., vol. 47, no. 4, pp. 374–385, 2011.
[3] P. Guderian and C. Kleinert, “Renewable energy for polar regions: A feasibility study,” Cold Reg. Sci. Technol., vol. 31, no. 3, pp. 231–240, 2000.
[4] R. Roura, “The footprint of Antarctic tourism: Policy changes and long-term management implications,” Polar Res., vol. 31, no. 1, p. 108, 2012.
[5] S. Brunet and D. Hourcard, “Renewable energy for polar research stations: An innovative strategy,” Renew. Energy Syst. Rev., vol. 24, no. 2, pp. 78–87, 2008.
[6] National Science Foundation, U.S. Antarctic Program: Final Environmental Impact Statement, Washington, DC:

NSF, 1996.
[7] L. Pyle, “South Pole Station: A history and overview,” Geophys. Monogr. Ser., 1999.
[8] H. van Loon, “Temperature fluctuations in the Antarctic,” Mon. Weather Rev., vol. 95, no. 12, pp. 701–705, 1967.
[9] J. Blunden and D. S. Arndt, “State of the climate in 2015,” Bull. Amer. Meteorol. Soc., vol. 97, no. 8, 2016.
[10] Amundsen-Scott South Pole Station – RESPEC.
Available: https://www.respec.com/project/amundson-scott-south-pole-station/.[Accessed: Jan. 3, 2025].
[11] B. Lazzarini, R. Gambelli, and M. Cerratti, “Solar and wind systems for Antarctic conditions,” Appl. Energy, vol. 102, pp. 892–901, 2012.
[12] NASA Surface Meteorology and Solar Energy. Available: http://eosweb.larc.nasa.gov/sse. [Accessed: Dec. 29, 2024].
[13] S. R. Wenham and M. A. Green, “Solar energy technologies: Advanced applications in polar climates,” Prog. Photovolt., vol. 6, no. 5, pp. 379–385, 1998.
[14] A. Waleed et al., “Study on hybrid wind-solar system for energy saving analysis in energy sector,” in Proc. 3rd Int. Conf. Comput. Math. Eng. Technol. (iCoMET), 2020, pp. 1–6.
[15] S. D. Al-Majidi, M. F. Abbod, and H. S. Al-Raweshidy, “A modified P&O-MPPT based on Pythagorean theorem and CV-MPPT for PV systems,” in *Proc. 53rd Int. Univ. Power Eng. Conf. (UPEC)*, 2018, pp. 1–6.
[16] A. Waleed, M. T. Riaz, M. F. Muneer, M. A. Ahmad, A. Mughal, M. A. Zafar, et al., “Solar (PV) water irrigation system with wireless control,” in Proc. 2019 Int. Symp. Recent Adv. Electr. Eng. (RAEE), 2019, pp. 1–4.
[17] G. K. Singh, “Solar power generation by PV (photovoltaic) technology: A review,” *Energy*, vol. 53, pp. 1–13, 2013.
[18] M. A. Enany, M. A. Farahat, and A. Nasr, “Modeling and evaluation of main maximum power point tracking algorithms for photovoltaics systems,” Renew. Sustain. Energy Rev., vol. 58, pp. 1578–1586, 2016.
[19] M. S. Ngan and C. W. Tan, “A study of maximum power point tracking algorithms for stand-alone photovoltaic systems,” in Proc. IEEE Appl. Power Electron. Colloq. (IAPEC), 2011, pp. 22–27.
[20] T. Esram and P. L. Chapman, “Comparison of photovoltaic array maximum power point tracking techniques,” IEEE Trans. Energy Convers., vol. 22, no. 2, pp. 439–449, Jun. 2007.
[21] R. Reisi, M. H. Moradi, and S. Jamasb, “Classification and comparison of maximum power point tracking techniques for photovoltaic system: A review,” Renew. Sustain. Energy Rev., vol. 19, pp. 433–443, Mar. 2013.
[22] M. A. A. M. Zainuri et al., “Adaptive P&O-fuzzy control MPPT for PV boost DC-DC converter,” in Proc. IEEE Int. Conf. Power Energy (PECon), 2012, pp. 2–5.
[23] R. Ramaprabha and B. L. Mathur, “Intelligent controller-based maximum power point tracking for solar PV system,” Int. J. Comput. Appl., vol. 12, no. 10, pp. 37–42, Dec. 2011.
[24] P. Q. Dzung, “The new MPPT algorithm using ANN-based PV,” in Proc. Int. Forum Strategic Technol., 2010, pp. 402–407.
[25] L. Jie and C. Ziran, “Research on the MPPT algorithms of photovoltaic system based on PV neural network,” in Proc. Chin. Control Decis. Conf. (CCDC), 2011, pp. 1851–1854.
[26] S. Premrudeepreechacharn and N. Patanapirom, “Solar-array modeling and maximum power point tracking using neural networks,” in Proc. IEEE Bologna Power Tech Conf., 2003, vol. 2, no. 3, pp. 419–423.
[27] S. E. K. T. Hiyama, “Artificial neural network-polar coordinated fuzzy controller-based maximum power point tracking control under partially shaded conditions,” Renew. Power Gener., vol. 3, no. 2, pp. 239–253, 2009.
[28] N. Femia et al., “Optimization of perturb and observe maximum power point tracking method,” IEEE Trans. Power Electron., vol. 20, no. 4, pp. 963–973, Jul. 2005.
[29] M. a. G. de Brito et al., “Main maximum power point tracking strategies intended for photovoltaics,” in *Proc. XI Brazilian Power Electron. Conf.*, 2011, pp. 524–530.
[30] M. Negnevitsky, Artificial Intelligence, 2nd ed. Hoboken, NJ: Pearson, 2005, pp. 1–415.
[31] J. Xu et al., “ANN based on IncCond algorithm for MPP tracker,” in Proc. 6th Int. Conf. Bio-Inspired Comput. Theor. Appl., 2011, vol. 3, pp. 129–134.
[32] A. M. Z. Alabedin et al., “Maximum power point tracking for photovoltaic systems using fuzzy logic and artificial neural networks,” in Proc. IEEE Power Energy Soc. Gen. Meeting, 2011, pp. 1–9.
[33] D. Mlakić and S. Nikolovski, “ANFIS as a method for determining MPPT in the photovoltaic system simulated in MATLAB/Simulink,” in Proc. 39th Int. Conv. Inf. Commun. Technol. Electron. Microelectron. (MIPRO), 2016, pp. 1082–1086.
[34] F. Khosrojerdi, S. Taheri, and A. Cretu, “An adaptive neuro-fuzzy inference system-based MPPT controller for photovoltaic arrays,” in Proc. IEEE Electr. Power Energy Conf. (EPEC), 2016, pp. 1–6.
[35] F. Belhachat and C. Larbes, “Global maximum power point tracking based on ANFIS approach for PV array configurations under partial shading conditions,” Renew. Sustain. Energy Rev., vol. 77, pp. 875–889, 2017.